UCN-2383
(3 11-60)

OAK RIDGE NATIONAL LABORATORY
Operated by
UNION CARBIDE NUCLEAR COMPANY
Division of Union Carbide Corporation
UCC
Post Office Box X
Oak Ridge, Tennessee

Syd Ball

~~METALLURGY DIVISION~~
File

For Internal Use Only

ORNL
CENTRAL FILES NUMBER
61-12-50

COPY NO. 31

DATE: December 26, 1961

SUBJECT: MSRE - Analog Computer Simulation of the System With a Servo Controller

TO: G. A. Cristy

FROM: O. W. Burke

ABSTRACT

One purpose of this study was to determine whether the fuel salt temperature inside the reactor could be controlled with a closed-loop servo controller. An "on-off" type controller was demonstrated using four different control signals. The stability of the system when using the controller was of primary interest.

These studies indicated that the system was stable for large and relatively fast power demand changes when using the controller with any one of the four control signals.

CONTENTS

I. Introduction: It is desirable to provide a controller for controlling the fuel temperature inside the reactor. There are many control concepts that would do the job.

The decision was made to try a simple "on-off" controller. E. R. Mann of the Instrumentation and Controls Division proposed four control signals which have definite possibilities and suggested that they be demonstrated on the analog computer. This report covers the analog computer demonstrations.

II. Description of the System Simulated: A schematic flow sheet of the MSRE system is shown in Figure 1. The temperature symbols are identified in Figure 2. The design information used in these studies is listed in Figure 3. The analog computer diagram is filed in the Engineering and Mechanical Division print files on Drawings 40331 and 40332.

The simulation of the thermal system and nuclear system as used in these studies has been discussed in previous preliminary reports.[1] There were two changes, however, that were significant. The temperature coefficient of reactivity of the graphite was changed from:

$$-2 \times 10^{-4} \frac{\delta K}{K\text{-}^{\circ}F} \quad \text{to} \quad -6 \times 10^{-5} \frac{\delta K}{K\text{-}^{\circ}F}$$

and the total secondary salt loop transit time was changed from 13 seconds to 24.2 seconds.

III. Description of Controller: The controller simulated was a simple "on-off" servo controller. The rod drive motor was a constant speed motor, driving the rods at a constant velocity sufficient to change the reactivity at a rate of:

$$.0002 \frac{\delta K}{K\text{-sec.}}$$

For the sake of simplicity, the rod worth was considered to be linear throughout the range used in these studies. The "time constant" of the controller was assumed to be 50 milliseconds. This "time constant" is the time required for the rod speed to attain 63% of full speed subsequent to receiving a demand signal to move the rods. The "dead band" of the controller was $\pm$ 2°F.

IV. Description of the Control Signals Used: The four different control signals used with the above described controller were as follows:

A. Control Signal No. 1, ϵ_1

The equation expressing ϵ_1 is as follows:

$$\frac{1}{G}\epsilon_1 = m \quad a\left\{\phi - \left(\left.T_o\right]_r - \left.T_i\right]_r\right) - g(t)\right\} + n\left\{\left(\left.T_o\right]_r + \left.T_i\right]_r\right) - 2T_{sp}\right\}$$

where,

G = control signal gain factor or amplification factor.

m, n, and a are constants that may be varied at will.

ϕ = neutron flux

$\left.T_o\right]_r$ = Fuel salt temperature at the reactor outlet.

$\left.T_i\right]_r$ = Fuel salt temperature at the inlet to the reactor.

$$g(t) = \lambda_2 \int_0^t \left[a\,\phi - \left(\left.T_o\right]_r - \left.T_i\right]_r \right) - g(t) \right] dt$$

This can be considered as a "reset mechanism." = [illegible]

T_{sp} - The desired mean fuel temperature in the reactor.

The controlled variable in ϵ_1 is the mean fuel temperature in the reactor, $\dfrac{\left.T_o\right]_r + \left.T_i\right]_r}{2}$. This variable appears only in the second term of the control signal. If this term alone is used as the control signal, the system is unstable.

The first term in ϵ_1 can be considered as a high frequency band pass stabilizing mechanism. It merely compares the rate of production of nuclear power to the rate of addition of heat to the fuel salt as it passes through the reactor. Note that for steady state operation:

$$\frac{d}{dt}\left[g(t)\right] = 0 = \lambda_2 \left[a\,\phi - \left(\left.T_o\right]_r - \left.T_i\right]_r \right) - g(t) \right]$$

$$g(t) = a\,\phi - \left(\left.T_o\right]_r - \left.T_i\right]_r \right)$$

This insures that the first term in ϵ_1 will be zero for steady state operation whether the term:

$$\left[a\,\phi - \left(\left.T_o\right]_r - \left.T_i\right]_r \right) \right]$$

is zero or not. For this reason, the constant, "a", does not have to be reset for various power levels. If ϵ_1 exceeds the dead band

positively, rods will be inserted and if ϵ_1 exceeds the dead band negatively, rods will be withdrawn. The analog computer diagram used to obtain ϵ_1 is shown in Figure 4.

The temperature sensing elements are thermocouples attached to the walls of the pipes containing the fluids whose temperatures are to be measured. There is a time lag between the time at which a change in temperature of the fluid occurs and the time at which this change is reflected in the thermocouple output signal. This time lag varies with different thermocouple designs, pipe wall thicknesses, etc. The time constant for this lag in the salt temperature thermocouples was designated as τ_1 and was considered to be 5 seconds.

The time constant of the g(t) circuit was arbitrarily chosen as 10 times that of the thermocouple. This long time constant was necessary in order to get "reset action" and still not interfere with the stabilizing effect during transients.

The other three control signals are quite similar to ϵ_1 and only their differences from ϵ_1 will be pointed out in the following descriptions of these signals.

B. <u>Control Signal No. 2, ϵ_2</u>.

The equation expressing ϵ_2 is as follows:

$$\frac{1}{G}\epsilon_2 = m\left\{a\,\phi - f_a\left(T_o\Big]_a - T_i\Big]_a\right) - g(t)\right\} + n\left\{\left(T_o\Big]_r + T_i\Big]_r\right) - 2T_{sp}\right\}$$

where,

f_a = air flow rate across the radiator

$T_o\Big]_a$ = outlet air temperature from radiator

$T_i\Big]_a$ = inlet air temperature to radiator

The time constant used for the air temperature sensing elements was 2.5 seconds and that used in the g(t) circuit was 25 seconds (τ_3 = 2.5 and λ_4 = 0.04).

Note that the controlled variable is the same as for ϵ_1. The stabilizing portion of the control signal is now formed by comparing the rate of production of power in the reactor to the rate of removal of power from the secondary salt by the air flowing across the radiator. Note that a multiplier is required in this circuit.

The analog computer diagram used to formulate ϵ_2 is shown in Figure 5.

C. Control Signal No. 3, ϵ_3 .

The equation expressing ϵ_3 is:

$$\frac{1}{G}\epsilon_3 = m\left\{a\ \phi - \left(T_i\Big]_s - T_o\Big]_s\right) - g(t)\right\} + n\left\{\left(T_c\Big]_r + T_i\Big]_r\right) - 2T_{sp}\right\}$$

where,

$T_i\Big]_s$ = secondary salt temperature at the radiator inlet

$T_o\Big]_s$ = secondary salt temperature at the radiator outlet

The controlled variable is the same as that in ϵ_1 and ϵ_2 . The stabilizing circuit is formed by comparing the rate of power production in the reactor to the rate of power loss of the secondary salt as it flows through the radiator. No multiplier is required since the flow rate in the secondary salt system is constant.

The "time constant" potentiometer settings are the same as those used in ϵ_1 . The analog computer diagram used to obtain ϵ_3 is shown in Figure 6.

D. Control Signal No. 4, ϵ_4 .

The equation describing ϵ_4 is:

$$\frac{1}{G}\epsilon_4 = m\left\{a\ \phi - \left(T_i\Big]_s - T_o\Big]_s\right) - g(t)\right\} + n\left(T_o\Big]_r - T_{sp}\right)$$

This control signal is the same as ϵ_3 except that a different controlled variable is used. The outlet fuel temperature from the reactor is the controlled variable. The analog computer diagram used to derive ϵ_4 is shown in Figure 7.

V. Procedure and Results: The system without a controller was shown to be unstable subsequent to any appreciable perturbation. The system was also shown to be unstable when using the controller with only the second term in the above control signals.

The stability of the system with the above controllers was checked subsequent to large changes in the power demand or load. The changes in the load for the four runs, each using one of the four above described control signals to the controller, were not precisely equal in magnitude and rate of change. The change in load was accomplished by manually turning a potentiometer. Also, no attempt was made to get optimum settings for M and N in each case. Therefore, the results cannot be compared quantitatively. In later runs linear ramp load changes will be used, and optimum

values of M and N used, so that controllers can be compared. Recordings of the controlled variable and the neutron flux were made subsequent to a load change, while using each of the four control signals to the controller. The conditions for these runs were as follows:

A. Using ϵ_1 as the control signal, M, as shown on the computer diagram, was set at .877 (quite arbitrarily) and N was set at 0.5. The load, or the heat removal rate by the air across the radiator, was set at approximately $\frac{1}{2}$ megawatt and the system permitted to stabilize. The load was increased from $\frac{1}{2}$ mw to 10 mw in 15 seconds, approximately at a constant rate. The curves obtained are shown in Figure 8. On all the curves only a relatively short time is shown. It can be seen that the curves are converging, which indicates stability.

B. Using ϵ_2 as the control signal, M, as shown on the computer diagram, was set at 0.877 and N set at 0.5. The load was changed from approximately 1.6 mw to 10 mw in 17 seconds. The resulting curves are shown in Figure 9.

C. Using ϵ_3 as the control signal, M, as shown on the computer diagram, was set at 0.25 and N was set at 0.5. The load was changed from approximately 1.6 mw to 10 mw in 13 seconds. The resulting curves are shown in Figure 10.

D. Using ϵ_4 as the control signal, M, as shown on the computer diagram, was set at 0.50 and N was set at 1.00. The load was changed from approximately 1.6 mw to 10 mw in 11 seconds. The resulting curves are shown in Figure 11.

The conclusion reached was that the system would be stable using the controller with any of the four control signals.

It should be pointed out that the constants M and N on the actual installation could be changed over a considerable range. No attempt was made to get the optimum settings on the computer, due to time limitations.

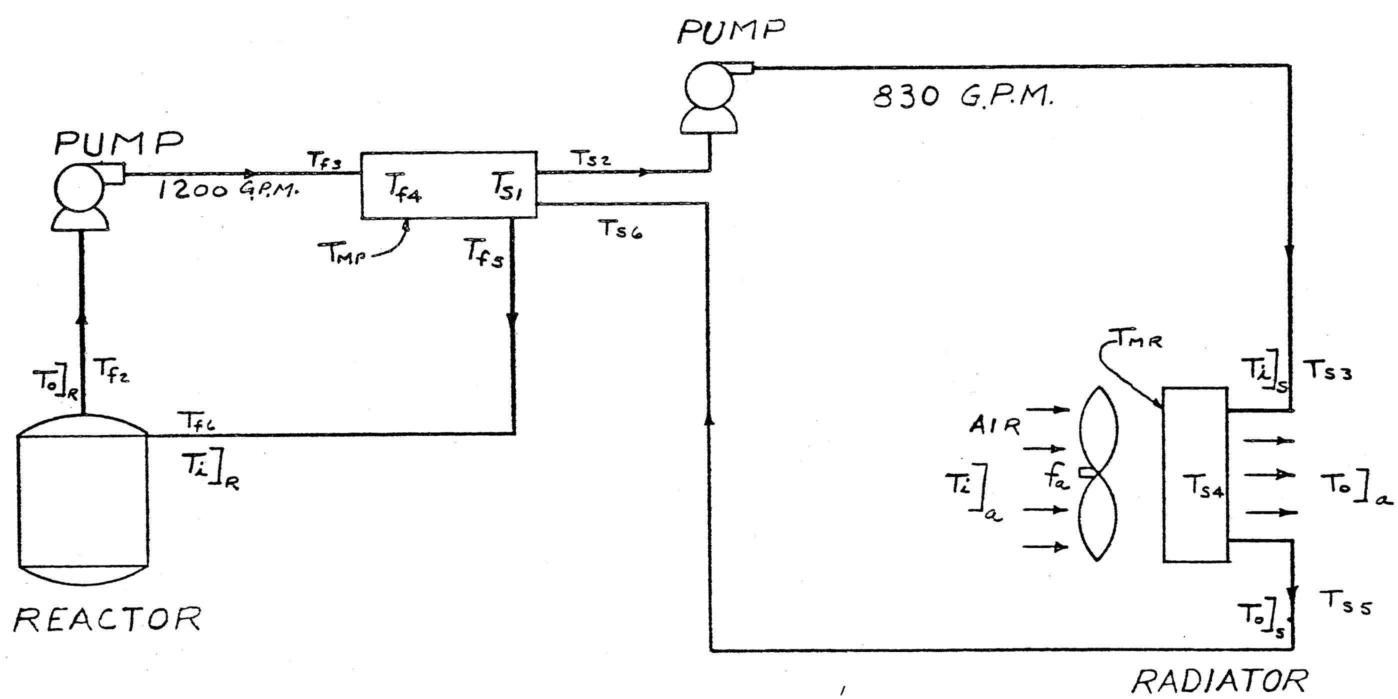

FIG. 1 BASIC FLOW DIAGRAM OF MSRE SYSTEM

Figure 2

IDENTIFICATION OF TEMPERATURE SYMBOLS

T_{f1}	-	Circulating fuel mean temperature in the reactor core.
T_{f2}	-	Circulating fuel temperature at the outlet of the reactor core.
T_{f3}	-	Circulating fuel temperature at the inlet to the primary heat exchanger.
T_{f4}	-	Circulating fuel mean temperature in the primary heat exchanger.
T_{f5}	-	Circulating fuel temperature at the outlet of the primary heat exchanger.
T_{f6}	-	Circulating fuel temperature at the inlet to the reactor core.
T_g	-	Mean temperature of the graphite in the reactor core.
T_{mp}	-	Mean temperature of the metal in the primary heat exchanger wall.
T_{s1}	-	Mean temperature of the secondary salt in the primary heat exchanger.
T_{s2}	-	Secondary salt temperature at the outlet of the primary heat exchanger.
T_{s3}	-	Secondary salt temperature at the inlet to the radiator.
T_{s4}	-	Mean temperature of the secondary salt in the radiator.
T_{s5}	-	Secondary salt temperature at the radiator outlet.
T_{s6}	-	Secondary salt temperature at the inlet to the primary heat exchanger.
T_{mr}	-	Mean temperature of the metal in the radiator.
$\overline{T}_{hot}$	-	Mean circulating fuel temperature in the "hot leg" of the primary system.
$\overline{T}_{cold}$	-	Mean circulating fuel temperature in the "cold leg" of the primary system.
T_{ma}	-	Mean air temperature in the radiator.

Figure 2 (contd.)

$T_i]_r$ - Fuel temperature at reactor core inlet.

$T_o]_r$ - Fuel temperature at reactor core outlet.

$T_i]_s$ - Secondary salt temperature at the radiator inlet.

$T_o]_s$ - Secondary salt temperature at the radiator outlet.

$T_i]_a$ - Cooling air temperature at radiator inlet.

$T_o]_a$ - Cooling air temperature at radiator outlet.

Figure 3

MSRE DESIGN POINT DATA AS OF 12-13-60

Reactor inlet temperature:	1175 °F
Reactor outlet temperature:	1225 °F
Mean graphite temperature: (with no fuel absorption)	1230 °F
Residence time in reactor:	7.63 sec.
Film drop from graphite to fuel:	Linear with power
Heat capacity of graphite:	0.425 $\frac{\text{BTU}}{\# \, ^\circ\text{F}}$
Prompt γ and neutron heating in graphite:	6% of 10 MW

Residence time in piping from reactor outlet to H. E. inlet	3.09 sec.
Residence time in H. E.	2.24 sec.
Heat capacity of metal in H. E.	200 BTU/°F
Avg. film drop between primary coolant and metal at D. P.	55.2 °F
Avg. drop in metal at D. P.	56.7 °F
Avg. film drop between metal and secondary coolant at D. P.	26.1 °F
Film drop between primary coolant and metal as function of flow: See graph, displace curve if necessary so that at 6.2 fps velocity $\Delta T = 55.2$ °F.	
Mean secondary coolant temperature at D. P.	1062 °F
Residence time in piping between H. E. outlet and reactor inlet (including coolant annulus)	9.04 sec.
Total circulation time	22.0 sec.

Temperature coefficient of reactivity of graphite:	$-6 \times 10^{-5}\ \delta K/K\text{-}^\circ F$
Temperature coefficient of reactivity of fuel:	$-3.3 \times 10^{-5}\ \delta K/K\text{-}^\circ F$
Melting point of primary coolant:	842 °F
Melting point of secondary coolant:	860 °F

Figure 3 (contd.)

Check points:

Thermal resistances: $\frac{\text{ft. hr. }^{\circ}\text{F}}{\text{BTU}}$

in primary coolant film:	3.28×10^{-4}
in metal:	3.32×10^{-4}
in secondary coolant film:	1.56×10^{-4}

Simulator data for secondary loop

Air temperature rise in radiator		200 °F
Air suction temperature		100 °F
Air flow		166,000 cfm (7.11×10^5 #/hr)
Heat capacity of radiator		242 BTU/°F
Heat capacity of secondary salt		0.57 $\frac{\text{BTU}}{\#\ ^{\circ}\text{F}}$
Density of secondary salt		120 #/ft^3
Residence times of secondary salt:		
in primary heat exchanger		1.75 sec.
in piping to radiator		5.20 sec.
in radiator		7.14 sec.
in piping from radiator		10.11 sec.
	Total	24.20 sec.
Residence time of air in radiator		0.01 sec.
Temperature differences in radiator:		
in salt film		13.4 °F
in tube wall		78.4 °F
in air film		770.7 °F

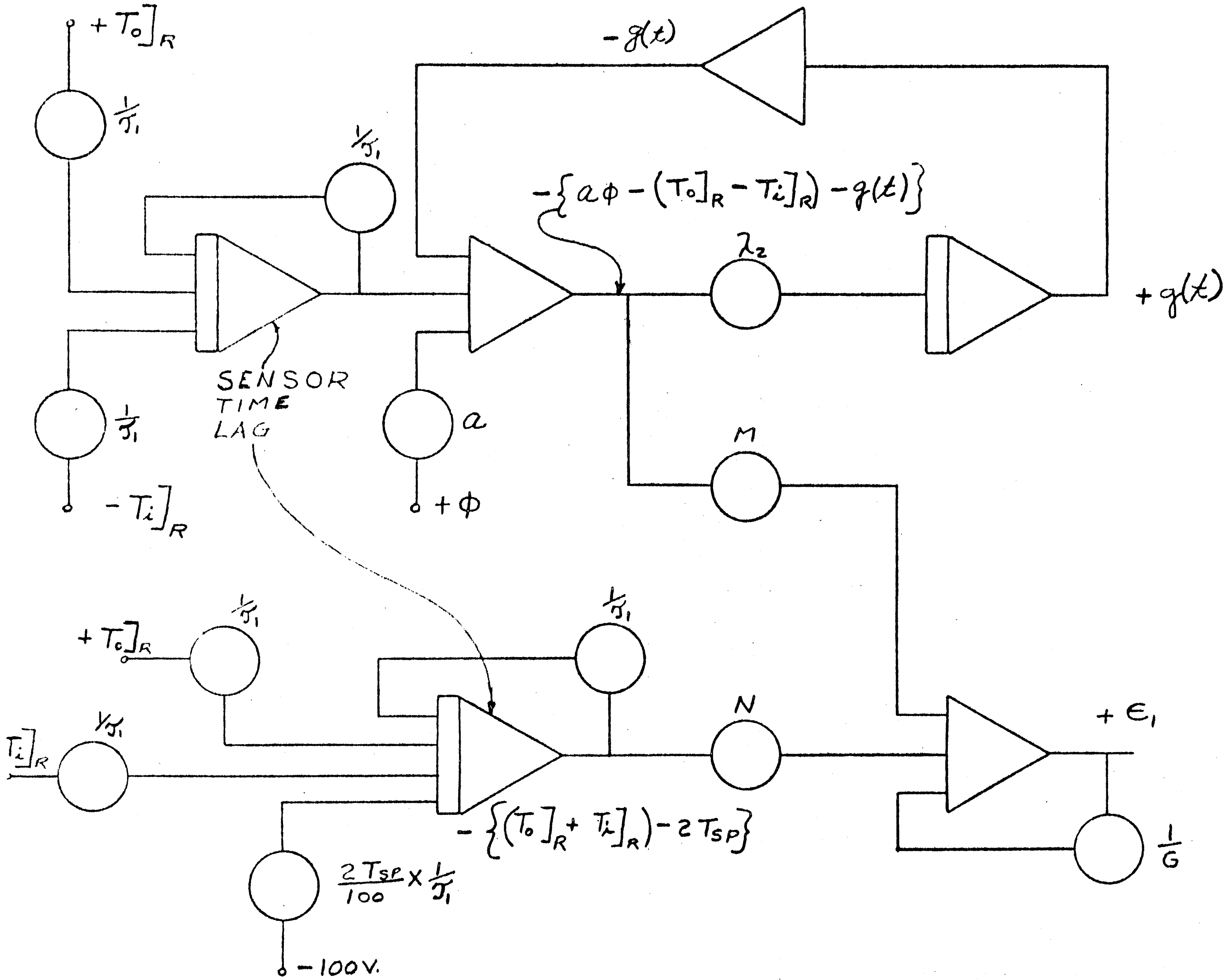

$$\lambda_2 \cong 0.1\left(\frac{1}{\tau_1}\right)$$

$$\frac{1}{G}\epsilon_1 = M\{a\phi - (T_o]_R - T_i]_R) - g(t)\} + N\{(T_o]_R + T_i]_R) - 2\,T_{SP}\}$$

FIG. 4. GENERATOR CIRCUIT FOR ϵ_1

ORNL-LR-Dwg. 64901
Unclassified

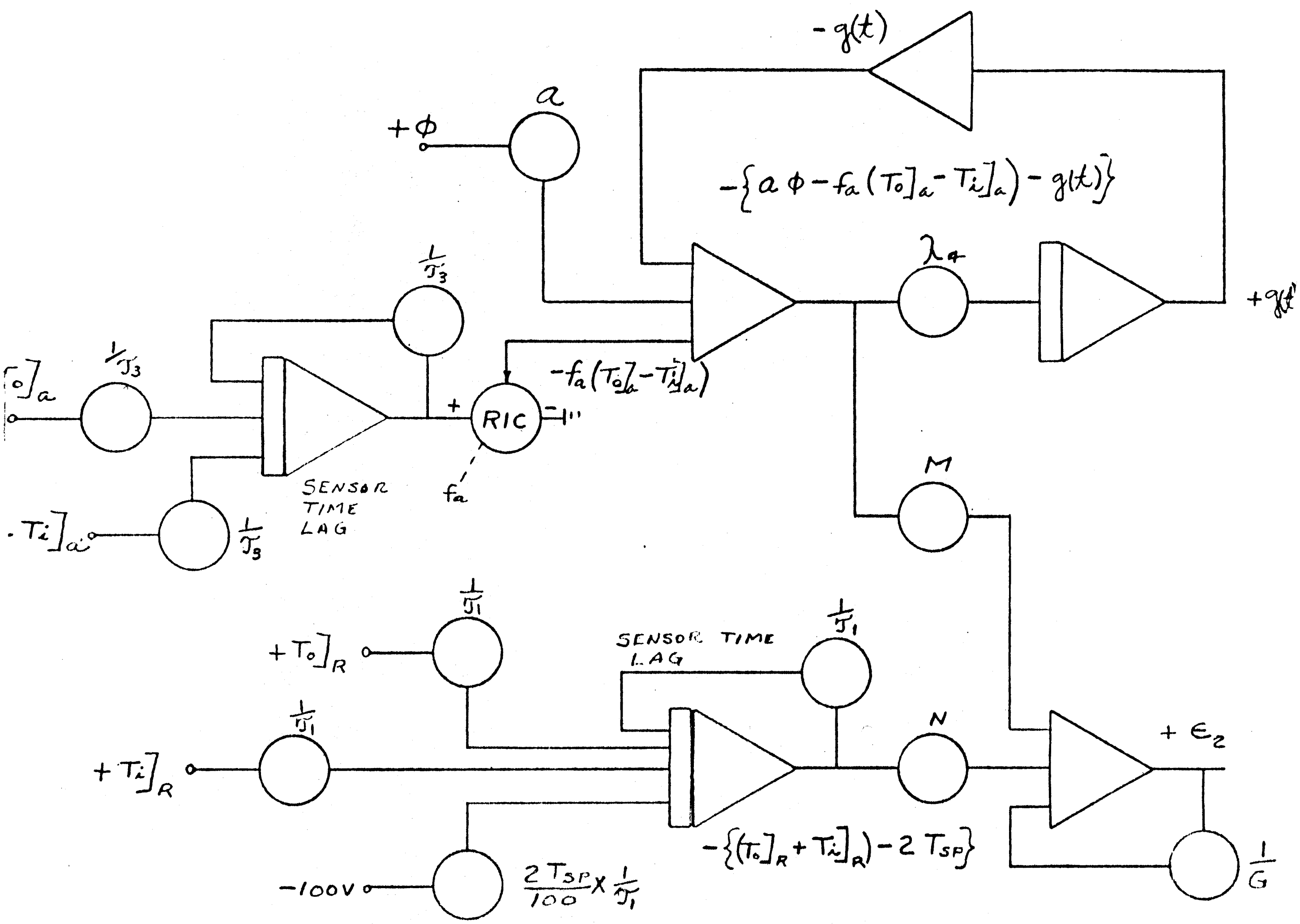

$$\lambda_4 \cong 0.1\left(1/T_3\right)$$

$$\frac{1}{G}\,\epsilon_2 = M\left\{a\phi - f_a\left(T_o]_a - T_i]_a\right) - g(t)\right\} + \left\{\left(T_o]_R + T_i]_R\right) - 2T_{SP}\right\} N$$

FIG. 5 GENERATOR CIRCUIT FOR ϵ_2.

Unclassified
ORNL-LR-Dwg. 64902

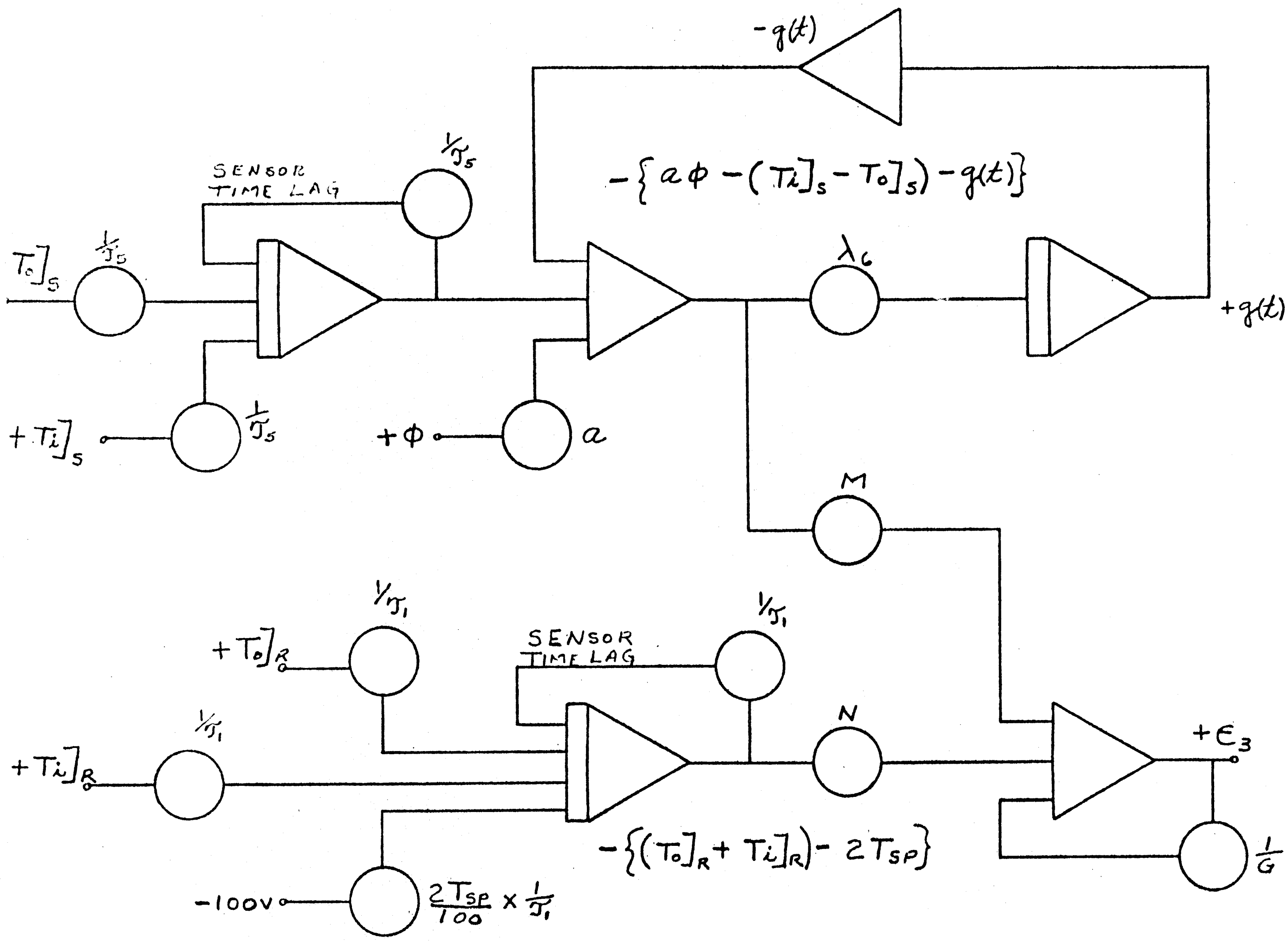

$$\lambda_6 \cong 0.1\left(\frac{1}{\tau_s}\right)$$

$$\frac{1}{G}\,\epsilon_3 = M\left\{a\phi - \left(T_i]_s - T_o]_s\right) - g(t)\right\} + N\left\{\left(T_o]_R + T_i]_R\right) - 2T_{SP}\right\}$$

FIG. 6 GENERATOR CIRCUIT FOR ϵ_3.

ORNL-LR-Dwg. 64903
Unclassified

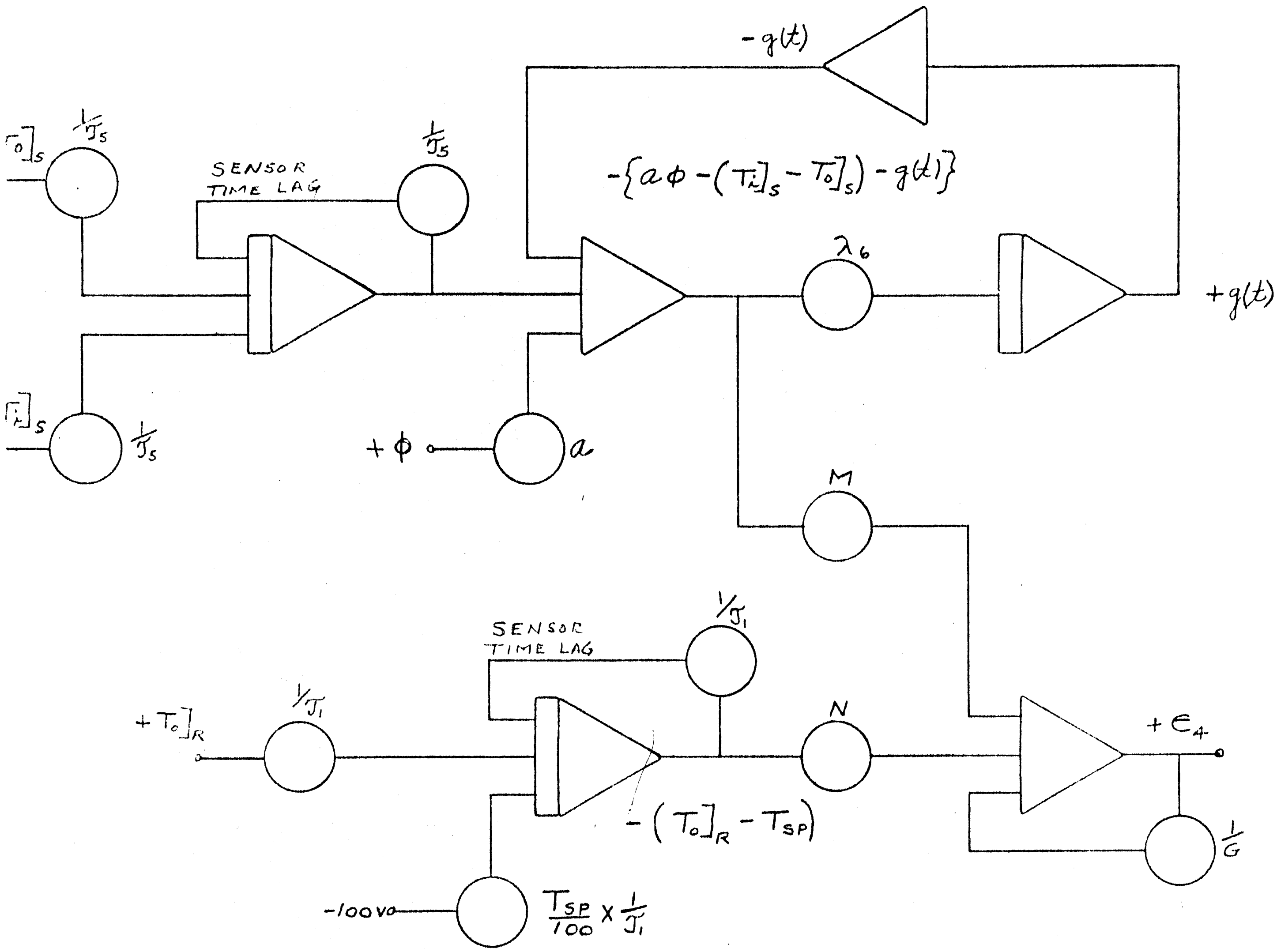

$$\lambda_6 \cong 0.1\left(\frac{1}{\tau_s}\right)$$

$$\frac{1}{G}\epsilon_4 = M\{a\phi - (T_i]_s - T_o]_s) - g(t)\} + N(T_o]_R - T_{SP})$$

FIG. 7 GENERATOR CIRCUIT FOR ϵ_4.

ORNL-LR-Dwg. 64904
Unclassified

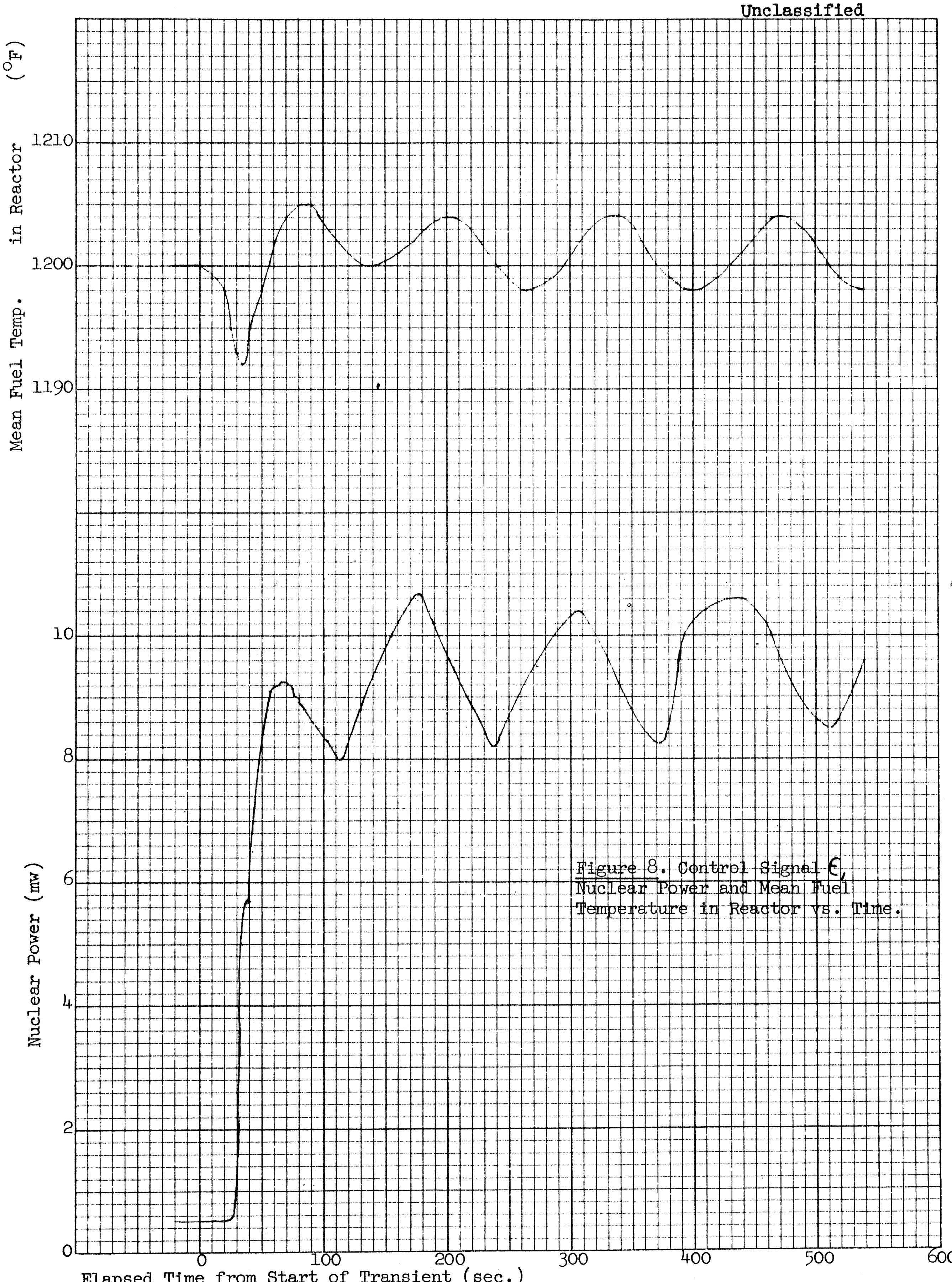

Figure 8. Control Signal ε, Nuclear Power and Mean Fuel Temperature in Reactor vs. Time.

P: 120 sec

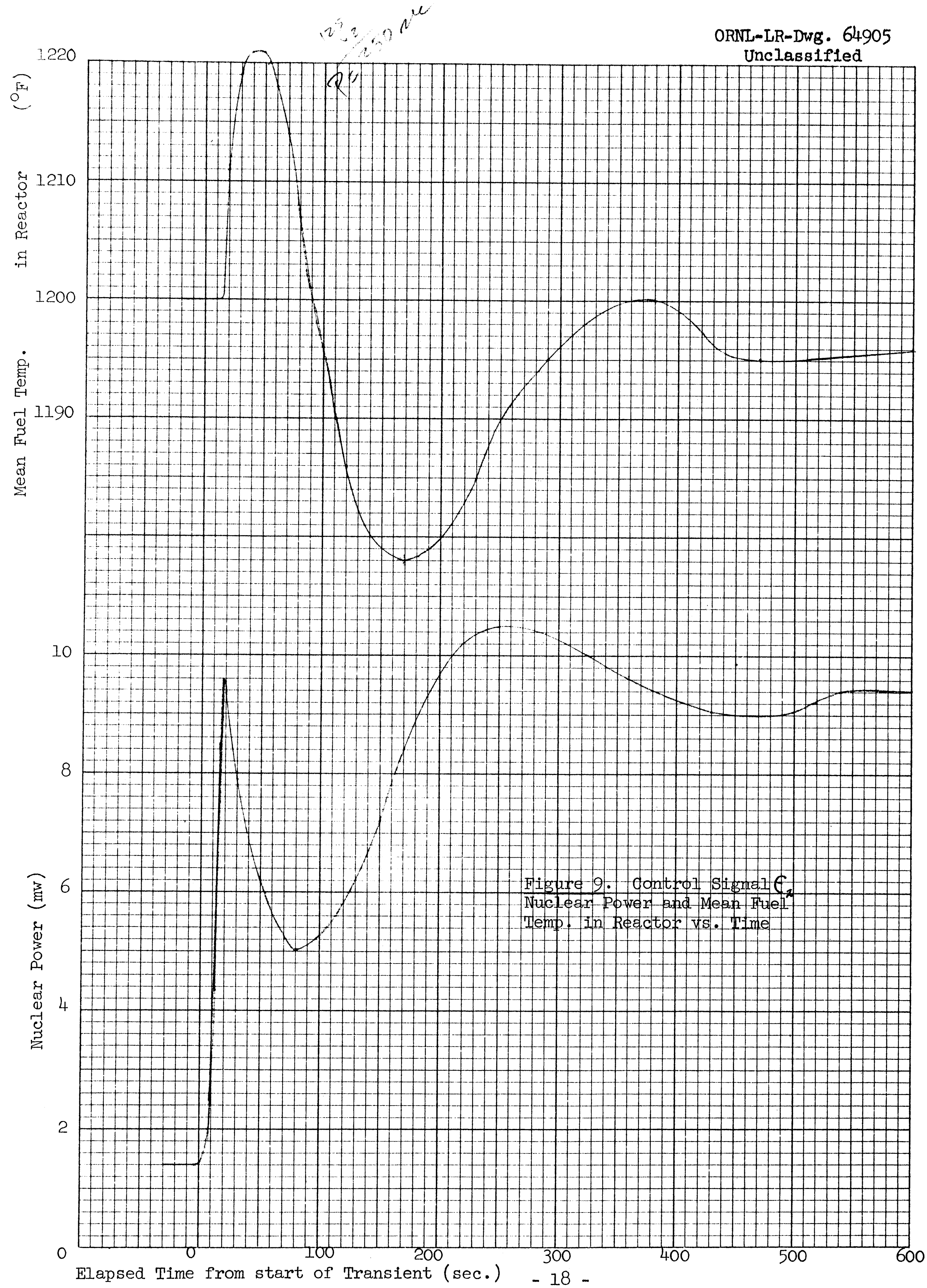

Figure 9. Control Signal ϵ_n Nuclear Power and Mean Fuel Temp. in Reactor vs. Time

ORNL-LR-Dwg. 64906
Unclassified

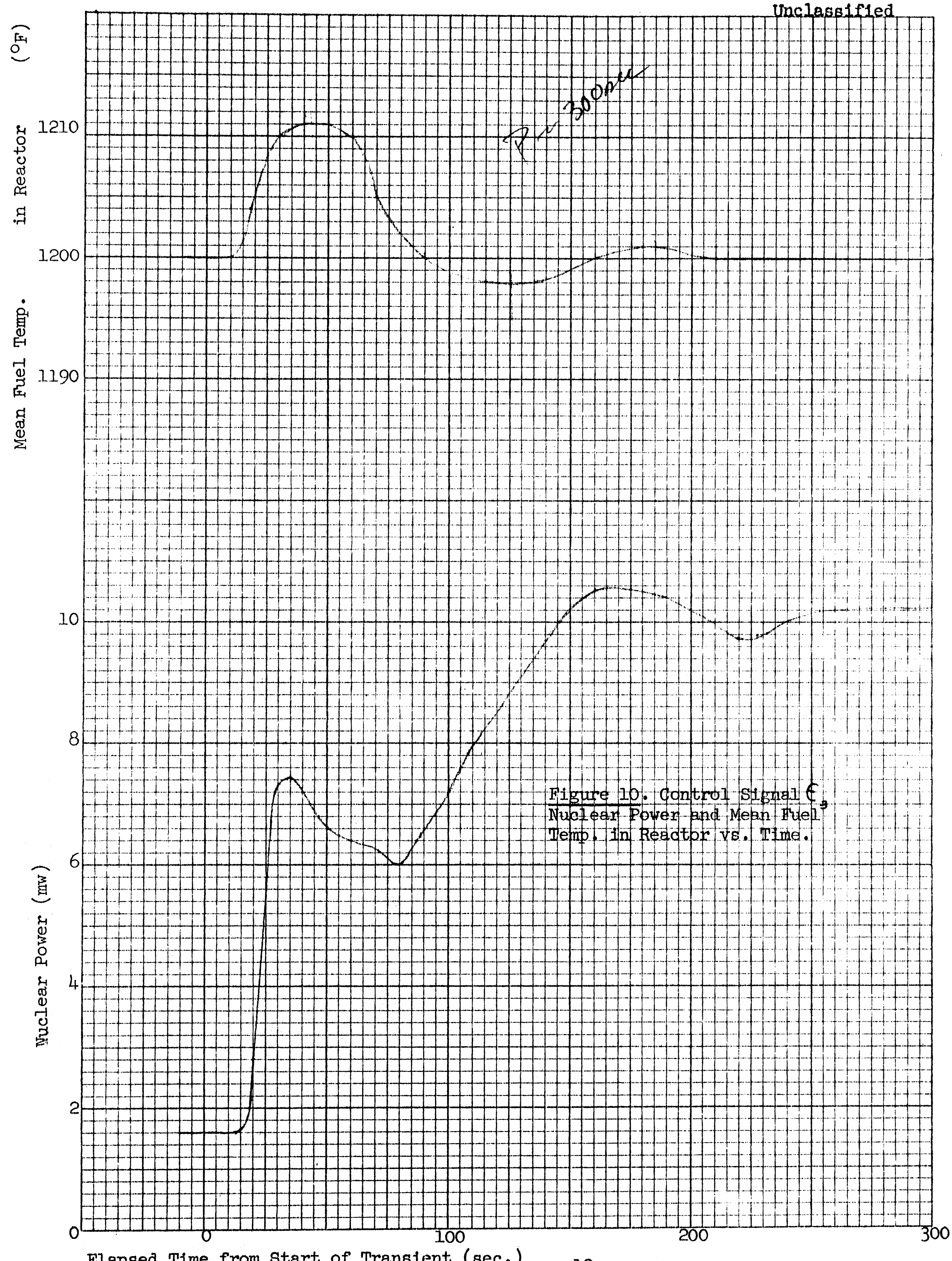

Figure 10. Control Signal ϵ_3 Nuclear Power and Mean Fuel Temp. in Reactor vs. Time.

ORNL-LR-Dwg. 64907
Unclassified

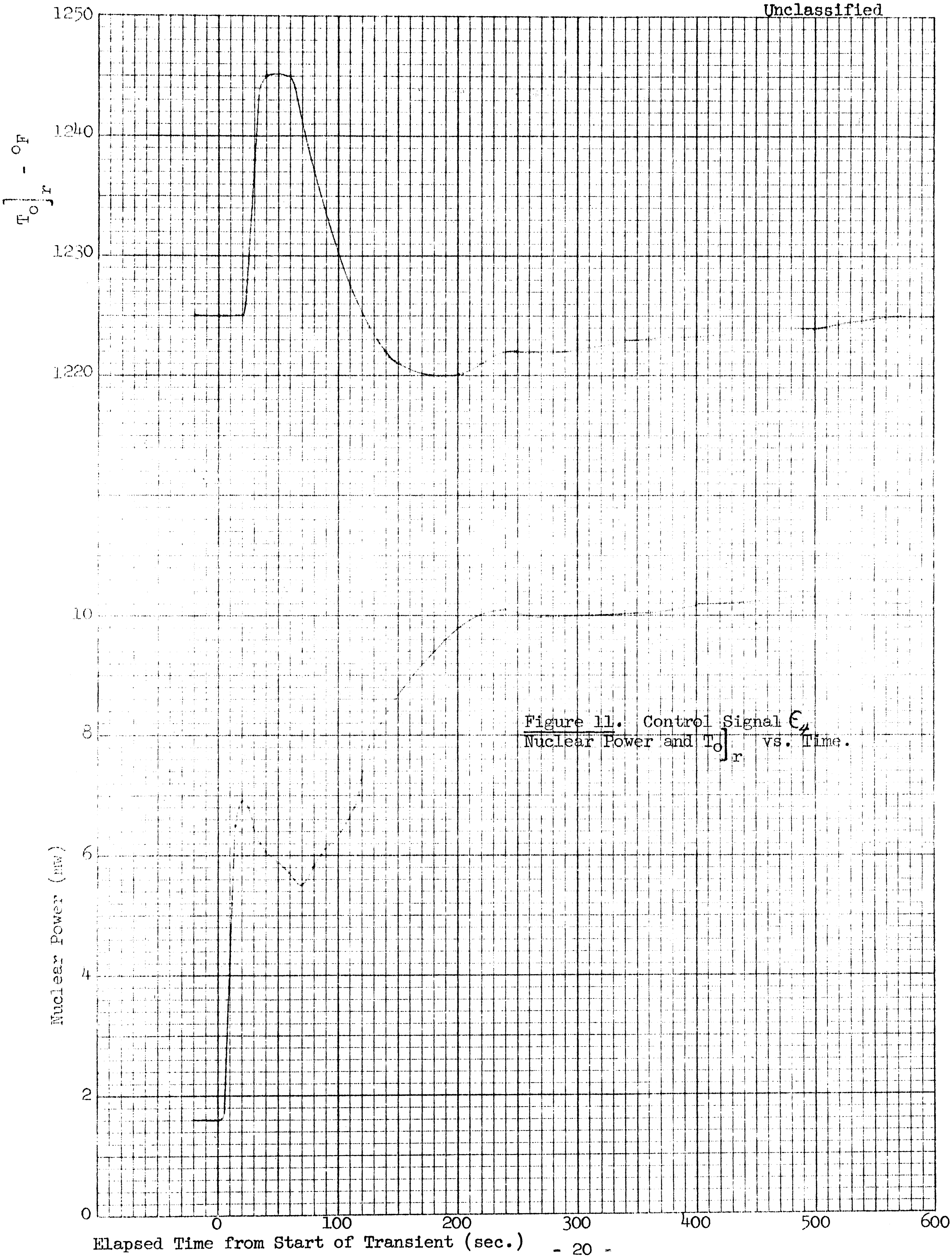

Figure 11. Control Signal ϵ_4 Nuclear Power and $T_o]_r$ vs. Time.

BIBLIOGRAPHY

1. O. W. Burke, MSRE - Preliminary Analog Computer Study - Flow Accident in Primary System, ORNL CF 60-6-110 (June 27, 1960)

O. W. Burke, MSRE - Analog Computer Simulation of a Loss of Flow Accident in the Secondary System and a Simulation of a Controller Used to Hold the Reactor Power Constant at Low Power Levels, ORNL CF 60-11-20 (Nov. 4, 1960)

O. W. Burke, MSRE - An Analog Computer Simulation of the System for Various Conditions - Progress Report No. 1, ORNL CF 61-3-42 (March 8, 1961)

DISTRIBUTION

1.	MSRP Director's Office	9204-1
2.	G. M. Adamson	2005
3.	L. G. Alexander	9204-1
4.	S. E. Beall	9204-1
5.	M. Bender	9201-3
6.	C. E. Bettis	1000
7.	E. S. Bettis	9204-1
8.	D. S. Billington	3025
9.	F. F. Blankenship	4500
10.	A. L. Boch	9204-1
11.	E. G. Bohlmann	9204-1
12.	S. E. Bolt	9204-1
13.	C. J. Borkowski	3500
14.	C. A. Brandon	9201-3
15.	F. R. Bruce	4500
16.	O. W. Burke	1000
17.	T. E. Cole	4500
18.	J. A. Conlin	9201-3
19.	W. H. Cook	2000
20.	G. A. Cristy	1000
21.	J. L. Crowley	9204-1
22.	F. L. Culler	4500
23.	J. H. DeVan	9201-3
24.	F. A. Doss	9201-3
25.	D. A. Douglas	2005
26.	N. E. Dunwoody	1000
27.	E. P. Epler	3500
28.	W. K. Ergen	4500
29.	D. E. Ferguson	4500
30.	A. P. Fraas	9704-1
31.	J. H. Frye	2000
32.	C. H. Gabbard	9201-3
33.	R. B. Gallaher	9204-1
34.	B. L. Greenstreet	9204-1
35.	W. R. Grimes	4500
36.	A. G. Grindell	9201-3
37.	R. H. Guymon	7500
38.	P. H. Harley	9204-1
39.	C. S. Harrill	3500
40.	P. N. Haubenreich	7500
41.	E. C. Hise	9204-1
42.	H. W. Hoffman	9204-1
43.	P. P. Holz	9204-1
44.	L. N. Howell	1000
45.	J. P. Jarvis	1000
46.	W. H. Jordan	4500
47.	P. R. Kasten	9204-1
48.	R. J. Kedl	9204-1
49.	G. W. Keilholtz	3550
50.	S. S. Kirslis	4500
51.	J. W. Krewson	9204-1
52.	J. A. Lane	4500
53.	W. J. Leonard	9204-1
54.	R. B. Lindauer	9204-1
55.	M. I. Lundin	9201-3
56.	R. N. Lyon	9204-1
57.	H. G. MacPherson	9704-1
58.	F. C. Maienschein	3010
59.	E. R. Mann	3500
60.	W. B. McDonald	9204-1
61.	H. F. McDuffie	4500
62.	C. K. McGlothlan	9204-1
63.	A. J. Miller	9704-1
64.	E. C. Miller	9204-1
65.	R. L. Moore	9204-1
66.	J. C. Moyers	9204-1
67.	C. W. Nestor	9204-1
68.	T. E. Northup	1000
69.	W. R. Osborn	9704-1
70.	L. F. Parsly	9204-1
71.	P. Patriarca	2005
72.	H. R. Payne	9204-1
73.	A. M. Perry	9204-1
74.	W. B. Pike	9201-3
75.	J. L. Redford	7500
76.	M. Richardson	9204-1
77.	R. C. Robertson	9204-1
78.	T. K. Roche	2000-A
79.	H. W. Savage	9201-3
80.	D. Scott	9204-1
81.	M. J. Skinner	4500
82.	G. M. Slaughter	2005
83.	A. N. Smith	9204-1
84.	P. G. Smith	9201-3
85.	I. Spiewak	9204-1
86.	B. Squires	9204-1
87.	J. A. Swartout	4500
88.	A. Taboada	9204-1
89.	J. R. Tallackson	9204-1
90.	R. E. Thoma	4500
91.	D. B. Trauger	9201-3
92.	W. C. Ulrich	9204-1

93.	B. S. Weaver	4500
94.	B. H. Webster	9204-1
95.	A. M. Weinberg	4500
96.	J. H. Westsik	9204-1
97.	L. V. Wilson	9201-3
98.	C. E. Winters	4500
99.	C. H. Wodtke	9204-1
100-101.	Reactor Div. Library (2)	9204-1
102-103.	Central Research Library (2)	4500
104.	Document Reference Library (1)	9711-1
105-107.	Laboratory Records (3)	4500
108.	Laboratory Records ORNL-RC	4500